



## Structure-based drug optimization and biological evaluation of tetrahydroquinolin derivatives as selective and potent CBP bromodomain inhibitors



Xiaoyang Bi<sup>a,b,i</sup>, Yu Chen<sup>b,c,i</sup>, Zhongya Sun<sup>c,d</sup>, Wenchao Lu<sup>e</sup>, Pan Xu<sup>b,c</sup>, Tian Lu<sup>c,f</sup>, Hong Ding<sup>b,c,\*</sup>, Naixia Zhang<sup>g</sup>, Hualiang Jiang<sup>b,c</sup>, Kaixian Chen<sup>b,c,h</sup>, Bing Zhou<sup>a,b,\*</sup>, Cheng Luo<sup>b,c,h,\*</sup>

<sup>a</sup> Department of Medicinal Chemistry, State Key Laboratory of Drug Research, Shanghai Institute of Materia Medica, Chinese Academy of Sciences, 555 Zuchongzhi Road, Shanghai 201203, China

<sup>b</sup> University of Chinese Academy of Sciences, 19 Yuquan Road, Beijing 100049, China

<sup>c</sup> Drug Discovery and Design Center, State Key Laboratory of Drug Research, Shanghai Institute of Materia Medica, Chinese Academy of Sciences, 555 Zuchongzhi Road, Shanghai 201203, China

<sup>d</sup> School of Life and Technology, Harbin Institute of Technology, Harbin 150001, China

<sup>e</sup> Department of Cancer Biology, Dana-Farber Cancer Institute, Boston, MA 02215, USA

<sup>f</sup> Jiangsu Key Laboratory for High Technology Research of TCM Formulae, Nanjing University of Chinese Medicine, 138 Xianlin Road, Nanjing 210023, China

<sup>g</sup> Department of Analytical Chemistry, Shanghai Institute of Materia Medica, Chinese Academy of Sciences, 555 Zuchongzhi Road, Shanghai 201203, China

<sup>h</sup> Open Studio for Druggability Research of Marine Natural Products, Pilot National Laboratory for Marine Science and Technology (Qingdao), 1 Wenhai Road, Aoshanwei, Jimo, Qingdao 266237, China

### ARTICLE INFO

#### Keywords:

Drug design

CBP

Bromodomain

Inhibitor

Acute myeloid leukemia

### ABSTRACT

CBP bromodomain could recognize acetylated lysine and function as transcription coactivator to regulate transcription and downstream gene expression. Furthermore, CBP has been shown to be related to many human malignancies including acute myeloid leukemia. Herein, we identified **DC-CPin734** as a potent CBP bromodomain inhibitor with a TR-FRET IC<sub>50</sub> value of 19.5 ± 1.1 nM and over 400-fold of selectivity against BRD4 bromodomains through structure based rational drug design guided iterative chemical modification endeavoring to discover optimal tail-substituted tetrahydroquinolin derivatives. Moreover, **DC-CPin734** showed potent inhibitory activity to AML cell line MV4-11 with an IC<sub>50</sub> value of 0.55 ± 0.04 μM, and its cellular on-target effects were further evidenced by c-Myc downregulation results. In summary, **DC-CPin734** showing good potency, selectivity and anti AML activity could serve as a potent and selective *in vitro* and *in vivo* probe of CBP bromodomain and a promising lead compound for future drug development.

CREB-binding protein (CREBBP, CBP) and its homologous Adenovirus E1A-associated 300-k<sub>D</sub> protein (EP300, P300) are two highly conserved mammalian histone acetyltransferases.<sup>1–3</sup> CBP/P300 contains a bromodomain which could act as a histone lysine acetylation “reader”.<sup>4</sup> CBP bromodomain as an important member of non-Bromodomain and Extraterminal domain (BET) family bromodomains could function as transcription co-activator to regulate transcription and gene expression. In particular, previous studies have shown that CBP bromodomain could regulate the expression of *MYC*,<sup>5,6</sup> a widely over-expressed oncogene in diverse human malignancies,<sup>7–9</sup> especially in hematologic malignancies,<sup>10,11</sup> suggesting CBP bromodomain inhibitors may serve as potential therapeutic agents for the treatment of

hematologic malignancies. Recently, CellCentric disclosed the development of CCS1477, which has nanomolar-level affinity for p300/CBP and is undergoing clinical trials in advanced prostate cancer,<sup>12,13</sup> multiple myeloma (MM), and acute myeloid leukemia (AML).<sup>14</sup> Due to the exclusive role of CBP in various pathways, there is still a desideration for new chemotypes of CBP Bromodomain inhibitors.

We recently identified **DC-CPin7** with tetrahydroquinolin methyl carbamate scaffold as a micromolar CBP bromodomain inhibitor through *in silico* screening (Fig. 1).<sup>15</sup> The co-crystal structure of **DC-CPin7** in complex with CBP bromodomain we obtained guided our iterative structure based chemical optimization. We identified two regions might be helpful to optimize our compounds: acetylated lysine

\* Corresponding authors at: University of Chinese Academy of Sciences, 19 Yuquan Road, Beijing 100049, China (H. Ding, B. Zhou and C. Luo).

E-mail addresses: [hding@simmm.ac.cn](mailto:hding@simmm.ac.cn) (H. Ding), [zhoubing@simmm.ac.cn](mailto:zhoubing@simmm.ac.cn) (B. Zhou), [cluoc@simmm.ac.cn](mailto:cluoc@simmm.ac.cn) (C. Luo).

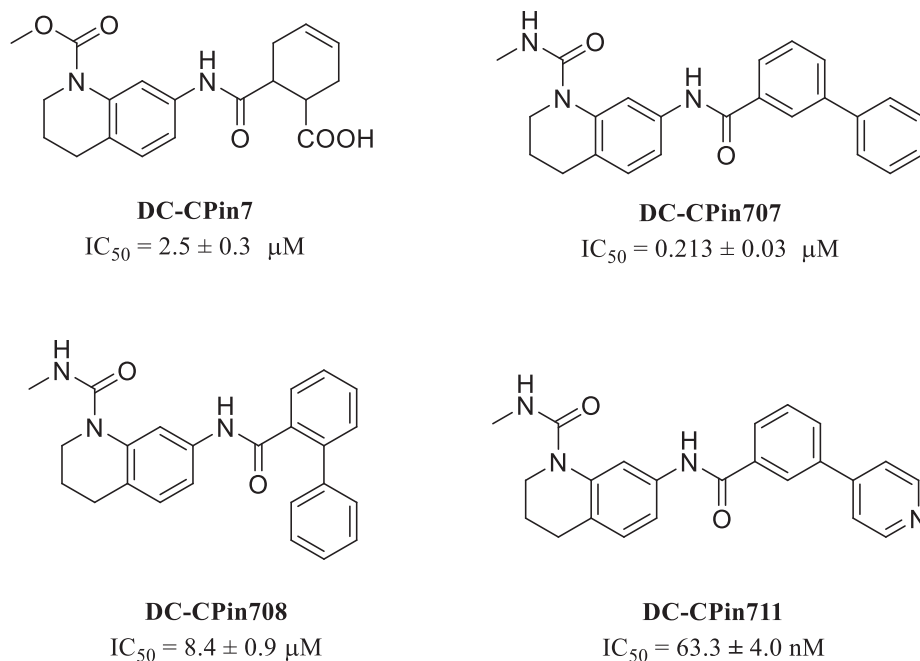
<sup>i</sup> These authors contributed equally.

<https://doi.org/10.1016/j.bmcl.2020.127480>

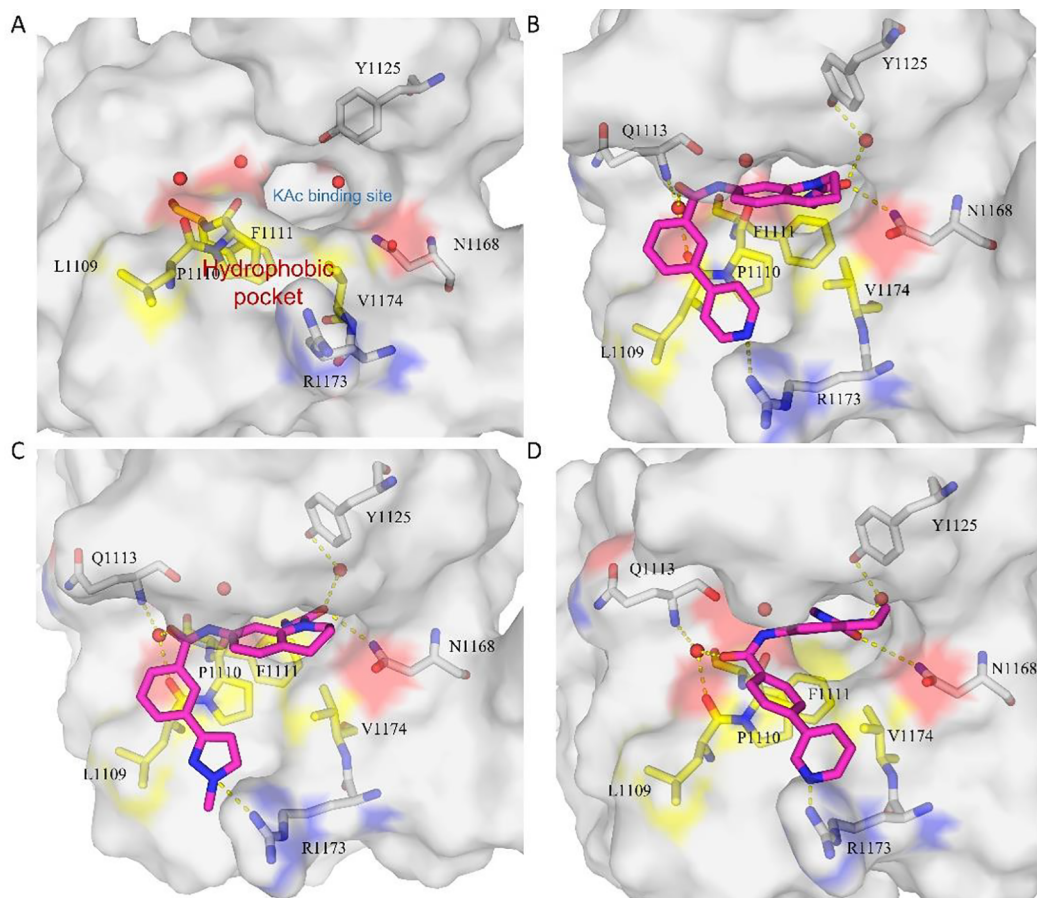
Received 7 June 2020; Received in revised form 22 July 2020; Accepted 6 August 2020

Available online 31 August 2020

0960-894X/ © 2020 Published by Elsevier Ltd.

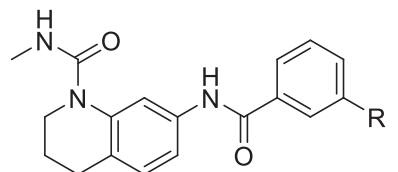


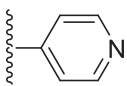
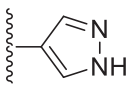
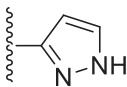
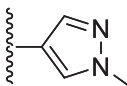
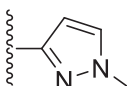
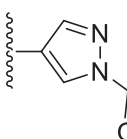
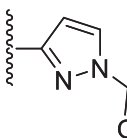
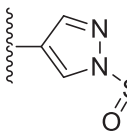
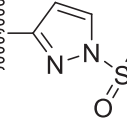
**Fig. 1.** Our previous reported tetrahydroquinolin derivatives as CBP bromodomain inhibitors.



**Fig. 2.** Molecular docking aided chemical modification of tetrahydroquinolin derivatives. (A) The surface animation of CBP bromodomain (PDB code 6LQX). Two important interacting regions were highlighted. Blue color represents positively charged group; red color represents negatively charged group; yellow color represents hydrophobic group. (B-D) Molecular docking results of CBP bromodomain with DC-CPin711, DC-CPin724 and DC-CPin731 respectively.

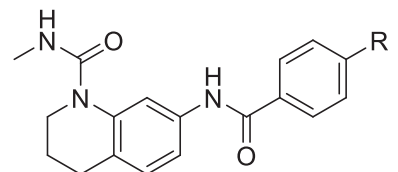
**Table 1**  
The inhibitory activities of heterocyclic derivatives based on DC-CPin711.

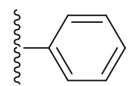
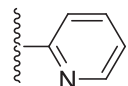
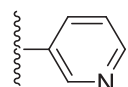
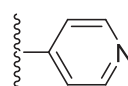


Compound	R	IC <sub>50</sub> (μM)
DC-CPin711		0.0633 ± 0.004
DC-CPin721		0.0913 ± 0.011
DC-CPin722		0.0929 ± 0.006
DC-CPin723		0.0554 ± 0.009
DC-CPin724		0.0457 ± 0.007
DC-CPin725		0.0765 ± 0.008
DC-CPin726		0.0946 ± 0.012
DC-CPin727		0.2861 ± 0.037
DC-CPin728		0.1032 ± 0.015

binding site and a hydrophobic pocket comprised of Leu1109, Pro1110, Phe1111 and Val1174 (Fig. 2A). First, we replaced chemically unstable *N*-methoxycarbonyl head with *N*-methylurea, the *in vitro* activity was maintained. Afterwards, we started to explore suitable substituents in the tail to increase interactions with residues in or around the hydrophobic pocket, among which DC-CPin711 making good van der Waals

**Table 2**  
The inhibitory activities of 4-position substituted derivatives.

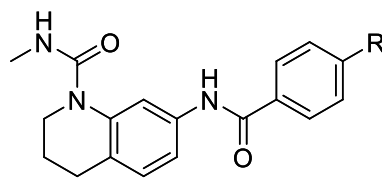


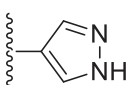
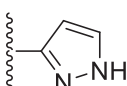
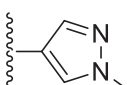
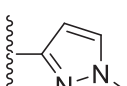
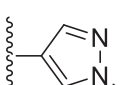
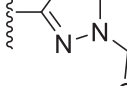
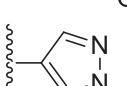
Compound	R	IC <sub>50</sub> (μM)
DC-CPin729		0.195 ± 0.009
DC-CPin730		0.102 ± 0.008
DC-CPin731		0.0537 ± 0.004
DC-CPin732		0.0892 ± 0.011

interactions with hydrophobic pocket and a weak hydrogen bond with CBP unique Arg 1173 showed an *in vitro* TR-FRET IC<sub>50</sub> value of 63.3 ± 4.0 nM and over 150-fold selectivity against BRD4 bromodomains. In this study, we utilized molecular docking aided structure-based optimization, combined with iterative organic synthesis trying to discover optimized tail-substituted tetrahydroquinolin derivatives with better *in vitro* and cellular potency and improved selectivity against BRD4 bromodomains.

The molecular docking results of DC-CPin711 displayed that the tail of DC-CPin711 was at the rim of the hydrophobic pocket and the nitrogen of pyridine was a bit far from Arg1173 with which a hydrogen bond was formed (Fig. 2B). Based on this, we adopted two strategies to seek suitable tail substituents to strengthen van der Waals interactions and hydrogen bond interaction with residues in or around the hydrophobic pocket. First we replaced the tail of DC-CPin711 with smaller heterocyclic analogues, as we expected smaller substituents on the tail could fit better in the hydrophobic pocket (Table 1). Indeed, pyrazol substituents DC-CPin723 (IC<sub>50</sub> = 0.0554 μM) and DC-CPin724 (IC<sub>50</sub> = 0.0457 μM) had an increase in potency over DC-CPin711. Molecular docking result of DC-CPin724 (Fig. 2C) revealed that the tail was sandwiched between Val1174 and Leu1109, while the phenyl ring and pyrazole ring made van der Waals interactions with the hydrophobic pocket formed by Leu1109, Pro1110 and Val1174. Meanwhile, the pyrazole ring sat in the hydrophobic pocket where nitrogen atom made a hydrogen bond with Arg1173 and formed a π stacking interactions with the pyrrolidinyl moiety of Pro1110. However, we observed a decrease in affinity when the pyrazol ring was acylated, which indicated the hydrogen bond receptor failed to enhance inhibitory potency but aggravated steric clash between the tail and the hydrophobic pocket (see Table 2).

**Table 3**  
The inhibitory activities of pyrazolyl analogues DC-CPin733-DC-CPin740.



Compound	R	IC <sub>50</sub> (μM)
DC-CPin733		0.0477 ± 0.004
DC-CPin734		0.0195 ± 0.001
DC-CPin735		0.0374 ± 0.004
DC-CPin736		0.0402 ± 0.003
DC-CPin737		0.0852 ± 0.005
DC-CPin738		0.0523 ± 0.007
DC-CPin739		0.0931 ± 0.010
DC-CPin740		0.0744 ± 0.004

Another strategy we took was to explore different substitute position in the tail to fully explore the optimal location of tail substituents to fit in the hydrophobic pocket. The results showed that phenyl ring substituted at 4-position (IC<sub>50</sub> = 0.1946 μM) was more potent than substituted at 2- or 3- position (we have reported 2- and 3- position substituted derivatives **DC-CPin707** and **DC-CPin708** with IC<sub>50</sub> values of 8.41 μM and 0.213 μM respectively). Moreover, with the substitution of pyridine at 4-position, there was a 2- to 4-fold increase in potency which suggested a hydrogen bond might be formed in the tail. Meanwhile, we noticed that **DC-CPin731**, the most potent 4-position

substituted pyridine derivative, had a higher affinity than the most potent 3-position substituted derivative **DC-CPin711**, indicating that substitution at 4-position might be more suitable for the tail sitting in the hydrophobic pocket. Docking results (Fig. 1D) showed that the tail of **DC-CPin731** was no longer clashed with the hydrophobic pocket, and both the phenyl and pyridyl moiety could made good van der Waals interactions with Leu1109, Pro1110 and Val1174. Furthermore, the tail formed a hydrogen bond with Arg1173 which was stronger than **DC-CPin711**, for 4-position substituted pyridine shorten the distance between the nitrogen atom and Arg1173. At this point, the two strategies we adopted were successful to improve potency.

Taken together, 5-membered heterocyclic substituents at the 4-position were synthesized to investigate the effects of the combination of these two strategies (Table 3). Gratifyingly, several highly potent compounds were identified through this modification. Among them, we managed to obtain **DC-CPin734** which had an IC<sub>50</sub> value of 0.0195 μM, a 2-fold improvement in potency over **DC-CPin724** and 2.5-fold over **DC-CPin731**. Docking result of **DC-CPin734** (Fig. 3A) showed that N-methylurea moiety occupied the KAc binding site, making multiple hydrogen bonds with Asn1168 and Tyr1125. The tail of **DC-CPin734** was sandwiched between Val1174 and Leu1109, while the phenyl ring and pyrazole ring sat in the center of the hydrophobic pocket formed by Leu1109, Pro1110 and Val1174, making strong van der Waals interactions. Meanwhile, the pyrazole ring sat in the hydrophobic pocket made a cation-π interaction with Arg1173 and formed a π stacking interactions with the pyrrolidiny moiety of Pro1110, of which the nitrogen atom formed a strong hydrogen bond with Arg1173. Taken together, the docking results rationalized the SAR and provided a reasonable binding mode for optimized compound **DC-CPin734**.

**Chemistry.** Consistent with what we reported before<sup>15</sup>, key intermediate compound **DC\_3** was prepared as depicted in Scheme 1. Treatment of tetrahydroquinoline **1** with 4-nitrophenyl chloroformate afforded **DC\_1**, then followed by methylamine hydrochloride gave urea **DC\_2**. Hydrogenation of **DC\_2** by Pd/C with H<sub>2</sub> yielded key intermediate **DC\_3** from which all the compounds were produced.

Amide coupling of **DC\_3** with 4-biphenylcarboxylic acid provided **DC-CPin729** in Scheme 2.

The synthesis of aryl analogues **DC-CPin723**, **24**, **30**, **31**, **32**, **35** and **36** is outlined in Scheme 3. Acids **CP\_01-CP\_07** were formed from Suzuki coupling of 3-Carboxyphenylboronic acid **11** or 4-Carboxyphenylboronic **12** acid with appropriate aryl bromides. Subsequent amide coupling with intermediate **DC\_3** yielded **DC-CPin723**, **DC-CPin724**, **DC-CPin730**, **DC-CPin731**, **DC-CPin732**, **DC-CPin735** and **DC-CPin736**.

The synthesis of aryl analogues **DC-CPin721**, **22**, **25**, **26**, **27**, **28**, **33**, **34**, **37**, **38**, **39** and **40** is outlined in Scheme 4. Amide coupling of **DC\_3** with 3 or 4-bromobenzoic acid provided **DC\_4** and **DC\_5**, respectively. From these intermediates, **DC-CPin721**, **22**, **33** and **34** could be accessed readily with Suzuki coupling of the appropriate boronic acid, then followed by acylation with acetyl chloride or methanesulfonyl chloride yielded **DC-CPin725- DC-CPin728** and **DC-CPin737- DC-CPin740**.

We utilized a couple of biophysical experiments to validate direct and strong binding of **DC-CPin734** to CBP bromodomain. The results of CPMG and STD NMR experiments ruling out false positive binding were included in Supplementary Information. Moreover, K<sub>d</sub> value of **DC-CPin734** binding to CBP bromodomain were measured by microscale thermophoresis (MST). The K<sub>d</sub> value calculated by a K<sub>d</sub> fitting model was 25.4 nM (Fig. 4), suggesting the strong binding of **DC-CPin734** to

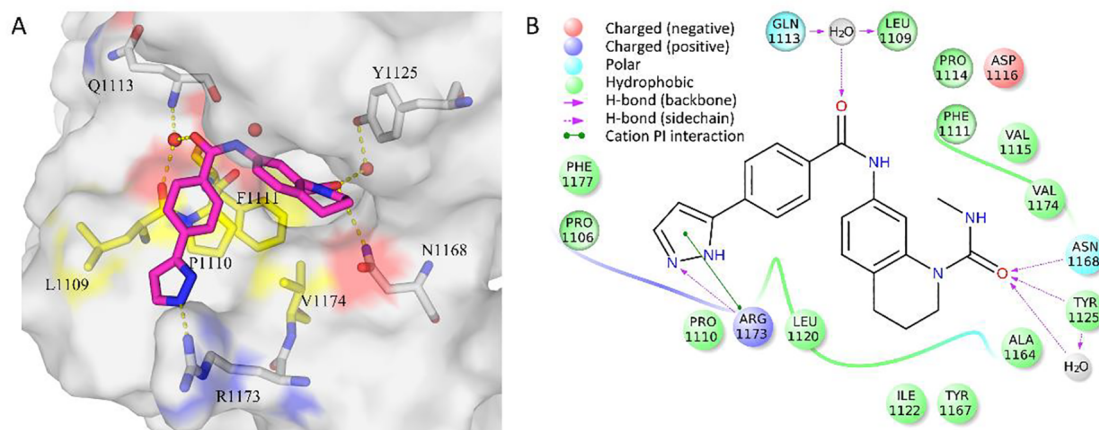
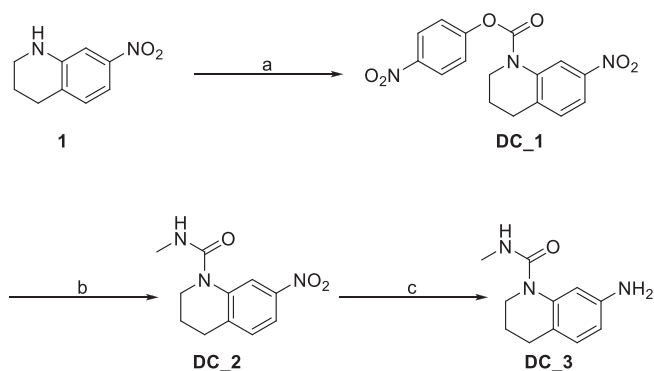
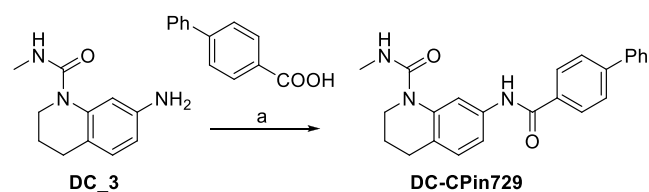


**Fig. 3.** The binding mode of DC-CPin734 to CBP bromodomain. (A) The 3D interaction map of DC-CPin734 with CBP bromodomain. (B) The 2D interaction map of DC-CPin734 with CBP bromodomain generated by Maestro.



**Scheme 1.** Synthesis of Key Intermediate DC<sub>3</sub>. Reagents and conditions: (a) 4-nitrophenyl chloroformate, TEA, DCM, 0 °C to rt; 70%; (b) methylamine hydrochloride, K<sub>2</sub>CO<sub>3</sub>, MeCN, 60 °C, 85%; (c) H<sub>2</sub>, Pd/C, MeOH, rt, 70%.



**Scheme 2.** Synthesis of Compounds DC-CPin729. Reagents and conditions: (a) DIPEA, HATU, DCM, rt, 53%.

CBP bromodomain.

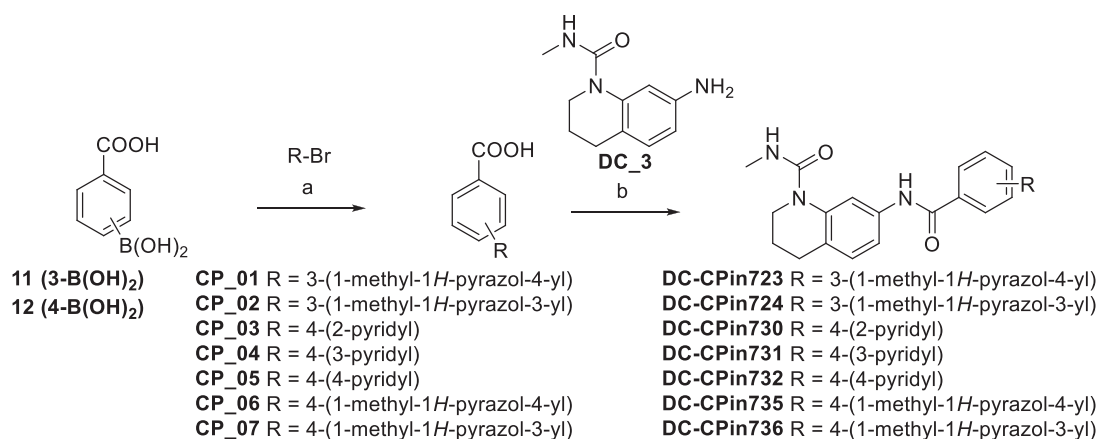
The selectivity of CBP bromodomain inhibitors against BET bromodomains has become a key issue of present CBP bromodomain inhibitor development. We used ALPHAScreen assays to test the inhibitory activities of DC-CPin734 to two BRD4 bromodomains. The result showed that DC-CPin734 showed over 400-fold selectivity against BRD4 bromodomains (Fig. 5). Arg1173 is a unique residue for CBP. A previous molecular dynamics and metadynamics simulations

study revealed that the hydrogen bond and cation- $\pi$  interaction between GSC-CBP30 and Arg1173 may be responsible for its selective binding.<sup>16</sup> As previous molecular docking analysis illustrated, the selectivity of DC-CPin734 against BRD4 bromodomains might partly due to the hydrogen bond and cation- $\pi$  interaction between DC-CPin734 and Arg1173.

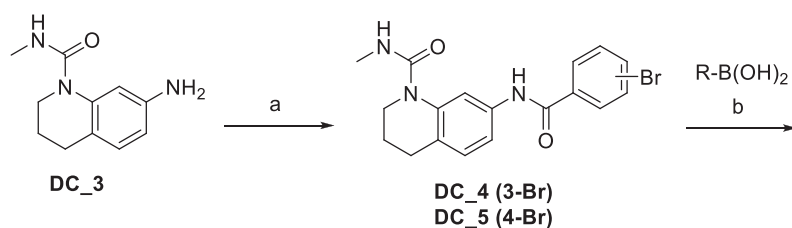
Since CBP has been identified to be closely involved in the occurrence and development processes in diverse human malignancies, we have evaluated the antitumor activities of tetrahydroquinolin derivative DC-CPin711 in 12 cancer cell lines, among which acute myeloid leukemia (AML) cell line MV4-11 was the most sensitive cell line evaluated.<sup>15</sup> Previous literature as well as our previous results have provided evidence of using CBP bromodomain inhibitors as potential therapeutic agents for the treatment of AML.<sup>11,17,18</sup> Therefore, cell viability of AML cell line MV4-11 was evaluated after 6.25  $\mu$ M or 1.56  $\mu$ M exposure of our tail-modified tetrahydroquinolin derivatives for 6 days. The IC<sub>50</sub> values of seven compounds showing over 50% of cell growth inhibition at 1.56  $\mu$ M were shown in the Table 4, indicating DC-CPin734 also showed best cellular anti-AML proliferation activity of compounds tested, which favors its cellular on-target effects.

Previous studies have shown that inhibition of the CBP bromodomain could regulate the expression level of c-Myc and thus alters downstream pathways.<sup>5,6,19</sup> The alterations of protein expression level of c-Myc after different concentrations (0, 0.25, 0.5, 1, 2  $\mu$ M) of DC-CPin734 treatments for 12 h were presented in Fig. 6. DC-CPin734 could significantly downregulate c-Myc expression levels at a dose-dependent manner in MV4-11 cell line, further suggesting the high on-target effects of DC-CPin734 in MV4-11 cell line.

We identified acetylated lysine binding site and a hydrophobic pocket in the co-crystal structure of DC-CPin7 in complex with CBP bromodomain might be helpful to optimize our compounds. Thereby, after *N*-methylurea head as acetylated lysine mimic was fixed, we focused on explore optimal substituents in the tail to increase interactions with residues in or around the hydrophobic pocket. Through molecular docking aided structure based rational drug design guided chemical modification, we optimized the tail from 3-position pyridyl derivatives to 4-position pyrazolyl substituents and eventually managed to obtain DC-CPin734 with a TR-FRET IC<sub>50</sub> value of 19.5  $\pm$  1.1 nM. The direct



**Scheme 3.** Synthesis of Compounds DC-CPin723, 24, 30, 31, 32, 35 and 36. Reagents and conditions: (a) DME/ water, Na<sub>2</sub>CO<sub>3</sub>, Pd(dppf)Cl<sub>2</sub>, 100 °C, 56–80%; (b) DIPEA, HATU, DCM, rt, 36–52%.



**Scheme 4.** Synthesis of Analogues DC-CPin721, 22, 25, 26, 27, 28, 33, 34, 37, 38, 39 and 40. Reagents and conditions: (a) 3-bromobenzoic acid or 4-bromobenzoic acid, DIPEA, HATU, DCM, rt, 65–74%; (b) MeCN/ water, K<sub>2</sub>CO<sub>3</sub>, sSPhos, allylpalladium(II) chloride dimer, 100 °C, 47–50%; (c) acetyl chloride or methanesulfonyl chloride, TEA, DCM, 0 °C to rt, 55–74%.

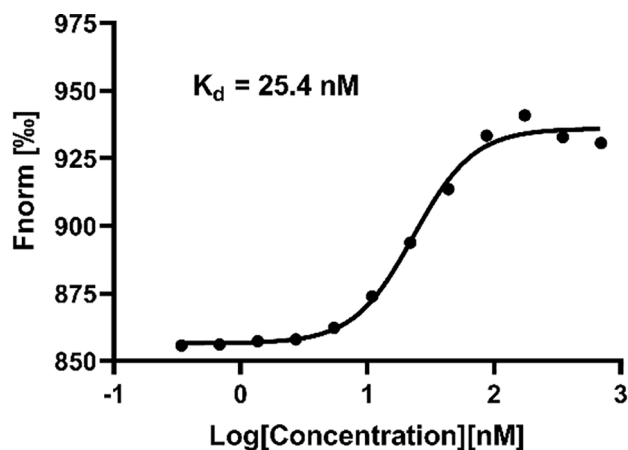
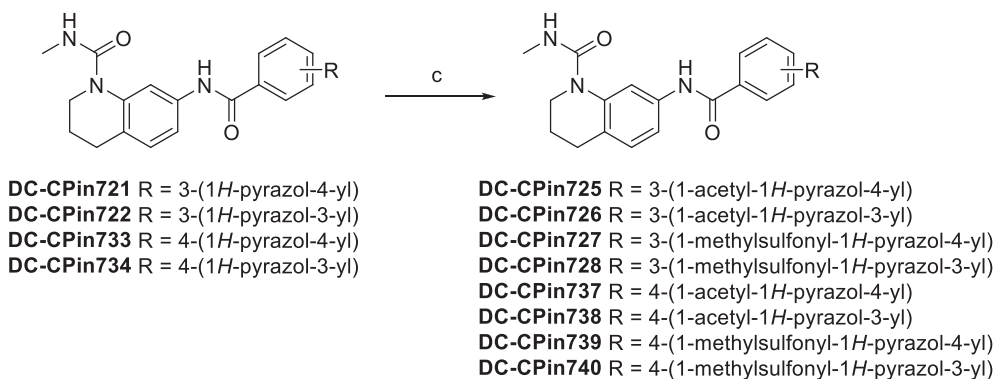


**Fig. 4.** The  $K_d$  fitting curve of DC-CPin734 binding to CBP bromodomain using  $K_d$  fitting model measured by microscale thermophoresis.

and strong binding of DC-CPin734 to CBP bromodomain was further confirmed by CPMG, STD NMR and MST biophysical experiments. Notably, DC-CPin734 showed over 400-fold selectivity to BRD4 bromodomains, which might be the result of introducing hydrogen bond and cation- $\pi$  interaction with CBP unique Arg1173. Moreover, DC-CPin734 showed potent inhibitory activity to AML cell line MV4-11 with an  $IC_{50}$  value of  $0.55 \pm 0.04 \mu\text{M}$ , and its cellular on-target effects were further evidenced by c-Myc downregulation results. In summary, DC-CPin734 could represent as a potent and selective *in vitro* and *in vivo* probe of CBP bromodomain and a promising lead compound for anti-AML drug development.

#### Declaration of Competing Interest

The authors declare that they have no known competing financial interests or personal relationships that could have appeared to influence the work reported in this paper.

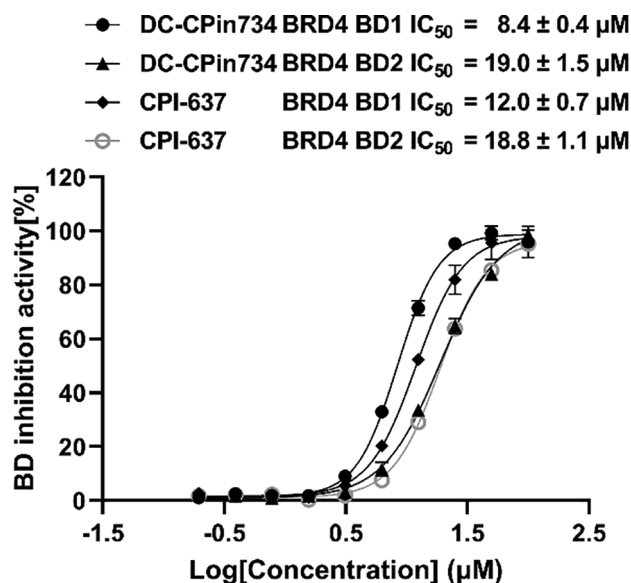


Fig. 5. The inhibitory activities of DC-CPin734 on two BRD4 bromodomains. CPI-637 was used as positive control.

Table 4

The inhibitory activities of tail-modified derivatives on MV4-11 cell line.

Compound	Inhibition rate (%) at 6.25 μM <sup>a</sup>	Inhibition rate (%) at 1.56 μM <sup>a</sup>	IC <sub>50</sub> (μM)
DC-CPin707	1.39	2.83	–
DC-CPin708	60.39	10.65	–
DC-CPin721	77.68	27.93	–
DC-CPin722	89.74	27.30	–
DC-CPin723	93.52	71.19	1.04 ± 0.07
DC-CPin724	99.50	70.52	0.98 ± 0.08
DC-CPin725	81.97	33.55	–
DC-CPin726	87.61	27.59	–
DC-CPin727	18.01	1.60	–
DC-CPin728	36.96	4.03	–
DC-CPin729	74.34	19.65	–
DC-CPin730	79.23	31.95	–
DC-CPin731	92.08	62.45	1.16 ± 0.08
DC-CPin732	88.66	37.61	–
DC-CPin733	98.28	73.45	0.87 ± 0.08
DC-CPin734	99.10	92.52	0.55 ± 0.04
DC-CPin735	94.41	77.35	0.73 ± 0.08
DC-CPin736	97.00	72.22	0.83 ± 0.1
DC-CPin737	83.76	23.93	–
DC-CPin738	91.35	35.84	–
DC-CPin739	40.17	4.50	–
DC-CPin740	57.24	8.81	–

<sup>a</sup>All inhibition rate values are reported as means of values from at least two determinations.

–: Less than 50% inhibition was observed at concentration of 1.56 μM.

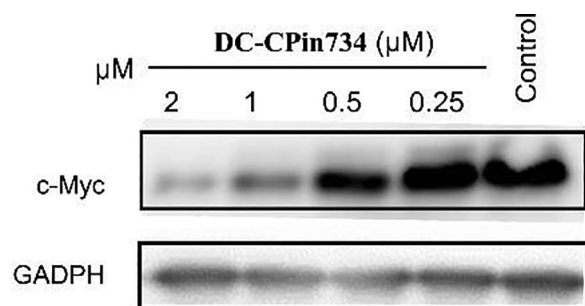


Fig. 6. The c-Myc protein expression levels after 12 h of DC-CPin734 treatment.

## Acknowledgements

We gratefully acknowledge financial support from the National Key R&D Program of China (2017YFB0202600 to H.D. and 2018YFA0508200 to B.Z.), the National Natural Science Foundation of China (21820102008 to H.J. and 81973166 to B.Z.), the National Science and Technology Major Project (2018ZX09711002 to H.J.), K.C. Wong Education Foundation to C.L., Science and Technology Commission of Shanghai Municipality (18431907100 to H.J., Y811298033 to Q.L. and 19XD1404700 to C.L.), the “Personalized Medicines Molecular Signature-based Drug Discovery and Development” (Strategic Priority Research Program of the Chinese Academy of Sciences, XDA12020368 to H.D.).

## Appendix A. Supplementary data

Supplementary data to this article can be found online at <https://doi.org/10.1016/j.bmcl.2020.127480>.

## References

- Bannister AJ, Kouzarides T. The CBP co-activator is a histone acetyltransferase. *Nature*. 1996;384(6610):641–643.
- Delvecchio M, Gaucher J, Aguilar-Gurrieri C, Ortega E, Panne D. Structure of the p300 catalytic core and implications for chromatin targeting and HAT regulation. *Nat Struct Mol Biol*. 2013;20(9):1040–1046.
- Mujtaba S, He Y, Zeng L, et al. Structural mechanism of the bromodomain of the coactivator CBP in p53 transcriptional activation. *Mol Cell*. 2004;13(2):251–263.
- Jain AK, Barton MC. Bromodomain histone readers and cancer. *J Mol Biol*. 2017;429(13):2003–2010.
- Faiola F, Liu X, Lo S, et al. Dual regulation of c-Myc by p300 via acetylation-dependent control of Myc protein turnover and coactivation of Myc-induced transcription. *Mol Cell Biol*. 2005;25(23):10220–10234.
- Conery AR, Centore RC, Neiss A, et al. Bromodomain inhibition of the transcriptional coactivators CBP/EP300 as a therapeutic strategy to target the IRF4 network in multiple myeloma. *Elife*. 2016;5.
- Tsuboi K, Hirayoshi K, Takeuchi K, et al. Expression of the c-myc gene in human gastrointestinal malignancies. *Biochem Biophys Res Commun*. 1987;146(2):699–704.
- Bieche I, Laurendeau I, Tozlu S, et al. Quantitation of MYC gene expression in sporadic breast tumors with a real-time reverse transcription-PCR assay. *Cancer Res*. 1999;59(12):2759–2765.
- Rochlitz CF, Herrmann R, deKant E. Overexpression and amplification of c-myc during progression of human colorectal cancer. *Oncology*. 1996;53(6):448–454.
- Dudley JP, Mertz JA, Rajan L, Lozano M, Broussard DR. What retroviruses teach us about the involvement of c-Myc in leukemias and lymphomas. *Leukemia*. 2002;16(6):1086–1098.
- Crawford TD, Romero FA, Lai KW, et al. Discovery of a potent and selective in vivo probe (GNE-272) for the bromodomains of CBP/EP300. *J Med Chem*. 2016;59(23):10549–10563.
- Breen ME, Mapp AK. Modulating the masters: chemical tools to dissect CBP and p300 function. *Curr Opin Chem Biol*. 2018;45:195–203.
- Brooks N, Prosser A, Young B, Gaughan L, Elvin P, Pegg N. CCS1477, a potent and selective p300/CBP bromodomain inhibitor, is targeted & differentiated from BET inhibitors in prostate cancer cell lines in vitro. *Cancer Res*. 2019;79(13).
- Brooks N, Raja M, Young BW, Spencer GJ, Somerville TC, Pegg NA. CCS1477: A Novel Small Molecule Inhibitor of p300/CBP Bromodomain for the Treatment of Acute Myeloid Leukaemia and Multiple Myeloma. *Blood*. 2019;134(Supplement\_1):2560–2560.
- Chen Y, Bi X, Zhang F, et al. Design, synthesis, and biological evaluation of tetrahydroquinolin derivatives as potent inhibitors of CBP bromodomain. *Bioorg Chem*. 2020;103991. <https://doi.org/10.1016/j.bioorg.2020.103991>.
- Wang QQ, An XL, Xu JH, et al. Classical molecular dynamics and metadynamics simulations decipher the mechanism of CBP30 selectively inhibiting CBP/p300 bromodomains. *Org Biomol Chem*. 2018;16(35):6521–6530.
- Hammitzsch A, Tallant C, Fedorov O, et al. CBP30, a selective CBP/p300 bromodomain inhibitor, suppresses human Th17 responses. *P Natl Acad Sci USA*. 2015;112(34):10768–10773.
- Zou LJ, Xiang QP, Xue XQ, et al. Y08197 is a novel and selective CBP/EP300 bromodomain inhibitor for the treatment of prostate cancer. *Acta Pharmacol Sin*. 2019;40(11):1436–1447.
- Vervoorts J, Luscher-Firzlaff JM, Rottmann S, et al. Stimulation of c-MYC transcriptional activity and acetylation by recruitment of the cofactor CBP. *Embo Rep*. 2003;4(5):484–490.